Computational Mechanics 31 (2003) 461–468 © Springer-Verlag 2003
DOI 10.1007/s00466-003-0450-3

# Solving anti-plane problems of piezoelectric materials by the Trefftz finite element approach

**Q.-H. Qin**



**Abstract** Applications of the Trefftz finite element method to anti-plane electroelastic problems are presented in this paper. A dual variational functional is constructed and used to derive Trefftz finite element formulation. Special trial functions which satisfy boundary conditions are also used to develop a special purpose element with local defects. The performance of the proposed element model is assessed by an example and comparison is made with results obtained by other approaches. The Trefftz finite element approach is demonstrated to be ideally suited for the analysis of the anti-plane problem.

**Keywords** Trefftz method, Piezoelectric, Anti-plane, Finite element

## 1 Introduction

During the past decades the hybrid-Trefftz finite element (FE) model, originating in 1977 [1], has been considerably improved and has now become a highly efficient computational tool for the solution of complex boundary value problems. Up to now, T-elements have been successfully applied to problems of elasticity [2, 3], Kirchhoff plates [4, 5], moderately thick Reissner-Mindlin plates [6–8], thick plates [9], general 3-D solid mechanics [10, 11], axisymmetric solid mechanics [12], potential problems [13, 14], shells [15], elastodynamic problems [16–18], transient heat conduction analysis [19], geometrically nonlinear plates [20–23] and materially nonlinear elasticity [24, 25]. Further, the concept of special purpose functions has been found to be of great efficiency in dealing with various geometry or load-dependent singularities and local effects (e.g., obtuse or reentrant corners, cracks, circular or elliptic holes, concentrated or patch loads) [2–4, 26, 27].

Planar crack problems have been examined by Sabino et al. [28] using the Trefftz boundary element method and by Freitas and Ji [29] using an equilibrium element model. In the present paper, we confine our attention to the applications of Trefftz FE method to anti-plane electroelastic problems. A pair of dual variational functionals is presented and used to derive the corresponding Trefftz FE formulation of piezoelectric materials. Special functions that satisfy traction-free conditions along crack faces are used as trial functions for those elements containing a crack. Numerical solutions to mode III problems obtained by the Trefftz FE method are compared with those obtained by other approaches.

*Received: 3 February 2003 / Accepted: 7 May 2003*

Q.-H. Qin
Department of Mechanics, Tianjin University,
Tianjin, 300072, China, School of AMME,
University of Sydney, Sydney, NSW 2006, Australia
E-mail: gin@mech.eng.usyd.edu.au

The work was performed under the auspices of an Australian Professorial Fellowship Program with grant number DP0209487 and 21st Century Education Promotion Key project from Tianjin University.

## 2 Basic formulations for anti-plane problem

### 2.1 Basic equations

In the case of anti-plane shear deformation involving only out-of-plane displacement $u_z$ and in-plane electric fields, we have

$$u_x = u_y = 0, \quad u_z = u_z(x,y), \quad \phi = \phi(x,y) \tag{1}$$

where $\phi$ is electrical potential. The differential governing equation can be written as

$$c_{44}\nabla^2 u_z + e_{15}\nabla^2\phi = 0, \quad e_{15}\nabla^2 u_z - \kappa_{11}\nabla^2\phi = 0 \quad \text{in } \Omega \tag{2}$$

with the constitutive equations

$$\begin{Bmatrix} \sigma_{xz} \\ \sigma_{yz} \\ D_x \\ D_y \end{Bmatrix} = \begin{bmatrix} c_{44} & 0 & -e_{15} & 0 \\ 0 & c_{44} & 0 & -e_{15} \\ e_{15} & 0 & \kappa_{11} & 0 \\ 0 & e_{15} & 0 & \kappa_{11} \end{bmatrix} \begin{Bmatrix} \gamma_{xz} \\ \gamma_{yz} \\ E_x \\ E_y \end{Bmatrix} \tag{3a}$$

or

$$\begin{Bmatrix} \gamma_{xz} \\ \gamma_{yz} \\ E_x \\ E_y \end{Bmatrix} = \begin{bmatrix} s_{44} & 0 & g_{15} & 0 \\ 0 & s_{44} & 0 & g_{15} \\ -g_{15} & 0 & \lambda_{11} & 0 \\ 0 & -g_{15} & 0 & \lambda_{11} \end{bmatrix} \begin{Bmatrix} \sigma_{xz} \\ \sigma_{yz} \\ D_x \\ D_y \end{Bmatrix} \tag{3b}$$

where $c_{44}$ is an elastic stiffness constant measured in a constant electric field while $\kappa_{11}$ stands for the dielectric constant measured at constant strain, $e_{15}$ is the piezoelectric constant, $\nabla^2 = \partial^2/\partial x^2 + \partial^2/\partial y^2$ is the two-dimensional Laplace operator, $\sigma_{xz}$ and $\sigma_{yz}$ are the shear stresses, $D_x$ and $D_y$ are the $x$- and $y$-components of electric displacement, $\gamma_{xz}, \gamma_{yz}$ and $E_x, E_y$ are, respectively, shear strains and electric fields given by

$$\gamma_{xz} = \frac{\partial u_z}{\partial x}, \quad \gamma_{xz} = \frac{\partial u_z}{\partial y}, \quad E_x = -\frac{\partial \phi}{\partial x}, \quad E_y = -\frac{\partial \phi}{\partial y} \ . \tag{4}$$

The constants $s_{44}, g_{15}$ and $\lambda_{11}$ are defined by the relations:

$$s_{44} = \frac{\kappa_{11}}{\Delta}, \ g_{15} = \frac{e_{15}}{\Delta}, \ \lambda_{11} = \frac{c_{44}}{\Delta}, \ \Delta = c_{44}\kappa_{11} + e_{15}^2 \ . \tag{5}$$

The boundary conditions of the boundary value problem (1)–(4) can be given by:



$$u_z = \bar{u}_z \quad \text{on} \quad \Gamma_u \tag{6}$$

$$t = \sigma_{3j} n_j = \bar{t} \quad \text{on} \quad \Gamma_t \tag{7}$$

$$D_n = D_i n_i = -\bar{\omega}_n = \bar{D}_n \quad \text{on} \quad \Gamma_D \tag{8}$$

$$\phi = \bar{\phi} \quad \text{on} \quad \Gamma_\phi \tag{9}$$

where $\bar{u}, \bar{t}, \bar{\omega}_n$ and $\bar{\phi}$ are, respectively, prescribed boundary displacement, traction vector, surface charge and electric potential, an overhead bar denotes prescribed value, $\Gamma = \Gamma_u + \Gamma_t = \Gamma_D + \Gamma_\phi$ is the boundary of the solution domain $\Omega$.

In the Trefftz FE form, Eqs. (1)–(9) should be completed by the following inter-element continuity requirements:

$$u_{ze} = u_{zf}, \quad \phi_e = \phi_f, \quad (\text{on } \Gamma_e \cap \Gamma_f, \text{conformity}) \ , \tag{10}$$

$$t_e + t_f = 0, \quad D_{ne} + D_{nf} = 0 \quad (\text{on } \Gamma_e \cap \Gamma_f, \text{traction reciprocity}) \ , \tag{11}$$

where '$e$' and '$f$' stand for any two neighbouring elements. Equations (1)–(11) are taken as a basis to establish the modified variational principle for Trefftz FE analysis of piezoelectric materials.

It is obvious from Eq. (2) that it requires

$$c_{44}\kappa_{11} + e_{15}^2 \neq 0 \tag{12}$$

to have non-trivial solutions for the out-of-plane displacement and in-plane electric fields. It results in

$$\nabla^2 u_z = 0, \quad \nabla^2 \phi = 0 \ . \tag{13}$$

## 2.2 Trefftz functions

It is well known that the solutions of the Laplace equation (13) may be found using the method of variable separation. By this method, the Trefftz functions are obtained as [14]:

$$u_z(r,\theta) = \sum_{m=0}^{\infty} r^m (a_m \cos m\theta + b_m \sin m\theta) \tag{14a}$$

$$\phi(r,\theta) = \sum_{m=0}^{\infty} r^m (c_m \cos m\theta + d_m \sin m\theta) \tag{14b}$$

for a bounded region and

$$u_z(r,\theta) = a_0^* + a_0 \ln r + \sum_{m=1}^{\infty} r^{-m} (a_m \cos m\theta + b_m \sin m\theta) \ , \tag{15a}$$

$$\phi(r,\theta) = c_0^* + c_0 \ln r + \sum_{m=1}^{\infty} r^{-m} (c_m \cos m\theta + d_m \sin m\theta) \tag{15b}$$

for an unbounded region, where $r$ and $\theta$ are a pair of polar coordinates. Thus, the associated T-complete sets of Eqs. (14) and (15) can be expressed in the form

$$T = \{1, r^m \cos m\theta, r^m \sin m\theta\} = \{T_i\} \ , \tag{16}$$

$$T = \{1, \ln r, r^{-m} \cos m\theta, r^{-m} \sin m\theta\} = \{T_i\} \ . \tag{17}$$

## 2.3 Assumed fields

To perform FE analysis, the solution domain $\Omega$ is divided into elements, and over each element '$e$', two independent fields are assumed in the following way:

(a) *The non-conforming intra-element field* is expressed by

$$\mathbf{u} = \begin{Bmatrix} u_z \\ \phi \end{Bmatrix} = \sum_{j=1}^{m} \begin{bmatrix} N_{1j} & 0 \\ 0 & N_{2j} \end{bmatrix} \begin{Bmatrix} c_{uj} \\ c_{\phi j} \end{Bmatrix} = \begin{bmatrix} \mathbf{N}_1 & 0 \\ 0 & \mathbf{N}_2 \end{bmatrix} \mathbf{c} = \mathbf{N}\mathbf{c} \tag{18}$$

where $\mathbf{c}$ is a vector of undetermined coefficient, $\mathbf{N}_i$ are taken from the component of the series (16) or (17), and $m$ is its number of components. The choice of $m$ has been discussed in Section 2.6 of Ref. [30]. For the reader's convenience, we described the basic rule for determining $m$ briefly. It is important to choose the proper number $m$ of trial functions $N_j$ for the Trefftz element with the hybrid technique. The basic rule used to prevent spurious energy modes is analogous to that in the hybrid-stress model. The necessary (but not sufficient) condition for the matrix $\mathbf{H}$, which is defined in Eq. (48) in Sect. 4 later, to have full rank is stated as [30]

$$2m \geq k - r \tag{19}$$

where $k$ and $r$ are numbers of nodal degrees of freedom of the element under consideration and of the discarded rigid body motion terms, or more generally the number of zero eigenvalues, ($r$ = 2 for the present anti-plane problem). Though the use of the minimum number $2m = k - r$ of flux mode terms in Eq. (19) does not always guarantee a stiffness matrix with full rank, full rank may always be achieved by suitably augmenting $m$. The optimal value of $m$ for a given type of element should be found by numerical experimentation.

(b) *An auxiliary conforming field*

$$\tilde{\mathbf{u}} = \begin{Bmatrix} \tilde{u}_z \\ \tilde{\phi} \end{Bmatrix} = \begin{bmatrix} \tilde{\mathbf{N}}_1 & 0 \\ 0 & \tilde{\mathbf{N}}_2 \end{bmatrix} \begin{Bmatrix} \mathbf{d}_u \\ \mathbf{d}_\phi \end{Bmatrix} + \begin{bmatrix} \tilde{\mathbf{N}}_{1c} & 0 \\ 0 & \tilde{\mathbf{N}}_{2c} \end{bmatrix} \begin{Bmatrix} \mathbf{d}_{uc} \\ \mathbf{d}_{\phi c} \end{Bmatrix} = \tilde{\mathbf{N}}\mathbf{d} + \tilde{\mathbf{N}}_c \mathbf{d}_c \ , \tag{20}$$

is independently assumed along the element boundary in terms of nodal DOF $\mathbf{d} = \{\mathbf{d}_u, \mathbf{d}_\phi\}^{\mathrm{T}}$ and $\mathbf{d}_c = \{\mathbf{d}_{uc}, \mathbf{d}_{\phi c}\}^{\mathrm{T}}$, where $\tilde{\mathbf{N}}$ represents the conventional finite element interpolating functions and $\tilde{\mathbf{N}}_{1c}, \tilde{\mathbf{N}}_{2c}$ are given in Eq. (20) below. For example, in a simple interpolation of the frame field on the side 1-C-2 of a particular element (Fig. 1), the frame functions are defined in the following way:

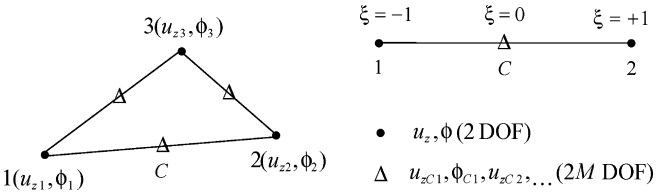


**Fig. 1.** Geometry of a triangular element

$$\tilde{u}_{z12} = \tilde{N}_1 u_{z1} + \tilde{N}_2 u_{z2} + \sum_{J=1}^{M_u} \xi^{J-1}(1-\xi^2) u_{zCJ} \ , \qquad (21a)$$

$$\tilde{\phi}_{12} = \tilde{N}_1 \phi_1 + \tilde{N}_2 \phi_2 + \sum_{J=1}^{M_\phi} \xi^{J-1}(1-\xi^2) \phi_{CJ} \ , \qquad (21b)$$

where $u_{zCJ}$ and $\phi_{CJ}$ are shown in Fig. 1, and

$$\tilde{N}_1 = \frac{(1-\xi)}{2}, \quad \tilde{N}_2 = \frac{(1+\xi)}{2} \ . \qquad (22)$$

Using the above definitions the generalized boundary forces and electric displacements can be derived from Eqs. (7), (8) and (18), denoting

$$\mathbf{T} = \begin{Bmatrix} t \\ D_n \end{Bmatrix} = \begin{Bmatrix} \sigma_{3j} n_j \\ D_j n_j \end{Bmatrix} = \begin{bmatrix} \mathbf{Q}_1 \\ \mathbf{Q}_2 \end{bmatrix} \mathbf{c} = \mathbf{Q}\mathbf{c} \ . \qquad (23)$$

## 2.4
## Special element containing angular corner

It is well known that singularities induced by local defects such as angular corners, cracks, and so on, can be accurately accounted for in the conventional FE model by way of appropriate local refinement of the element mesh. However, an important feature of the Trefftz element method is that such problems can be far more efficiently handled by the use of special purpose functions [4]. Elements containing local defects (see Fig. 2) are treated by simply replacing the standard regular functions **N** in Eq. (18) by appropriate special purpose functions. One common characteristic of such trial functions is that it is not only the governing differential equations, which are Laplace equations here, which are satisfied exactly but also some prescribed boundary conditions at a particular portion $\Gamma_{eS}$ (see Fig. 2) of the element boundary. This enables various singularities to be specifically taken into account without troublesome mesh refinement. Since the whole element formulation remains unchanged (except that now the frame function $\tilde{\mathbf{u}}$ in Eq. (19) is defined and the boundary integration is performed only at the portion $\Gamma_{e^*}$ of the element boundary $\Gamma_e = \Gamma_{e^*} + \Gamma_{eS}$, see Fig. 2) [4], all that is needed to implement the elements containing such special trial functions is to provide the element subroutine of the standard, regular elements with a library of various optional sets of special purpose functions.

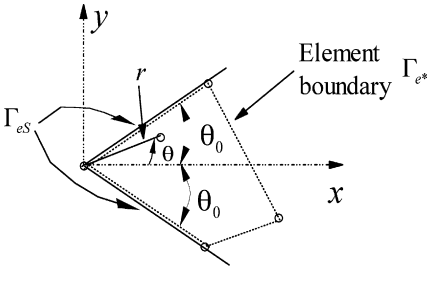


**Fig. 2.** Special element containing a singular corner

In this section we show how special purpose functions can be constructed to satisfy both the Laplace equation (13) and the traction-free boundary conditions on angular corner faces (Fig. 2). The derivation of such functions is based on the general solution of the two-dimensional Laplace equation:



$$u_z(r,\theta) = a_0 + \sum_{n=1}^{\infty} (a_n r^{\lambda_n} + b_n r^{-\lambda_n}) \cos(\lambda_n \theta) + \sum_{n=1}^{\infty} (d_n r^{\lambda_n} + e_n r^{-\lambda_n}) \sin(\lambda_n \theta) \ , \qquad (24)$$

$$\phi(r,\theta) = e_0 + \sum_{n=1}^{\infty} (e_n r^{\lambda_n} + f_n r^{-\lambda_n}) \cos(\lambda_n \theta) + \sum_{n=1}^{\infty} (g_n r^{\lambda_n} + h_n r^{-\lambda_n}) \sin(\lambda_n \theta) \ . \qquad (25)$$

Appropriate trial functions for a singular corner element are obtained by considering an infinite wedge (Fig. 2) with particular boundary conditions prescribed along the sides $\theta = \pm\theta_0$ forming the angular corner. The boundary conditions on the upper and lower surfaces of the wedge are free of surface traction and surface charge:

$$\sigma_{r\theta} = c_{44} \frac{\partial u_z}{r \partial \theta} + e_{15} \frac{\partial \phi}{r \partial \theta} = 0, \quad D_\theta = e_{15} \frac{\partial u_z}{r \partial \theta} - \kappa_{11} \frac{\partial \phi}{r \partial \theta} = 0 \ . \qquad (26)$$

This leads to

$$\frac{\partial u_z}{\partial \theta} = 0, \quad \frac{\partial \phi}{\partial \theta} = 0 \quad (\text{for } \theta = \pm\theta_0) \ . \qquad (27)$$

To solve this problem, we rewrite the general solution (24) as

$$u_z(r,\theta) = a_0 + \sum_{n=1}^{\infty} (a_n r^{\lambda_n} + b_n r^{-\lambda_n}) \cos(\lambda_n \theta) + \sum_{n=1}^{\infty} (d_n r^{\beta_n} + e_n r^{-\beta_n}) \sin(\beta_n \theta) \qquad (28)$$

where $\lambda_n$ and $\beta_n$ are two sets of constants which are assumed to be greater than zero. Differentiating solution (28) and substituting it into Eq. (27) yields

$$\frac{\partial u_z}{\partial \theta}\Big|_{\theta=\pm\theta_0} = -\sum_{n=1}^{\infty} \lambda_n (a_n r^{\lambda_n} + b_n r^{-\lambda_n}) \sin(\pm\lambda_n \theta_0) + \sum_{n=1}^{\infty} \beta_n (d_n r^{\beta_n} + e_n r^{-\beta_n}) \cos(\pm\beta_n \theta_0) = 0 \ . \qquad (29)$$

Since the solution must be limited for $r = 0$, we should specify

$$b_n = e_n = 0 \ . \qquad (30)$$

From Eq. (29) it can be deduced that

$$\sin(\pm\lambda_n\theta_0)=0,\quad \cos(\pm\beta_n\theta_0)=0\ , \tag{31}$$

leading to

$$\lambda_n\theta_0=n\pi,\quad (n=1,2,3,\ldots)\ , \tag{32}$$

$$2\beta_n\theta_0=n\pi,\quad (n=1,3,5,\ldots)\ . \tag{33}$$

Thus, for an element containing an edge crack (in this case $\theta_0=\pi$), the solution can be written in the form



$$u_z(r,\theta)=a_0+\sum_{n=1}^{\infty}a_n r^n\cos(n\theta)+\sum_{n=1,3,5}^{\infty}d_n r^{\frac{n}{2}}\sin\left(\frac{n}{2}\theta\right)\ . \tag{34}$$

With solution (34), the internal function defined in Eq. (18) can be taken as

$$N_{2n-1}=r^n\cos(n\theta),\ \ N_{2n}=r^{(2n-1)/2}\sin\left(\frac{(2n-1)}{2}\theta\right),\quad (n=1,2,3,\ldots)\ . \tag{35}$$

It is obvious that the displacement function (34) includes the term proportional to $r^{1/2}$, whose derivative is singular at the crack tip. The solution for the second equation of (27) can be obtained similarly.

## 3 Modified variational principle

As mentioned in [30], in FE analysis physical fields, such as displacements or other desired unknown parameters, are obtained by way of minimizing an energy functional. In general, the energy functional consists of all the energies associated with the particular FE model. The minimum of the functional is found by setting the derivative of the functional with respect to the unknown nodal point parameters to zero. In view of this understanding, a variational functional used for deriving Trefftz FE formulation may be constructed in such a way that the stationary conditions of the functional satisfy Eqs. (6)–(11) for the category of Trefftz-displacement formulation, as Eq. (13) is satisfied, a priori, through use of the assumed field (18). For the boundary value problem described by Eqs. (1)–(13), the corresponding dual variational functional is constructed in the form

$$\Pi_m^{\sigma D}=\sum_e\Pi_{me}^{\sigma D}=\sum_e\Big\{\Pi_e^{\sigma D}-\int_{\Gamma_{De}}(\bar{D}_n-D_n)\tilde{\phi}\ \mathrm{d}s-\int_{\Gamma_{te}}(\bar{t}-t)\tilde{u}_z\ \mathrm{d}s+\int_{\Gamma_{Ie}}(D_n\tilde{\phi}+t\tilde{u}_z)\mathrm{d}s\Big\} \tag{36a}$$

$$\Pi_m^{\varepsilon E}=\sum_e\Pi_{me}^{\varepsilon E}=\sum_e\Big\{\Pi_e^{\varepsilon E}+\int_{\Gamma_{\phi e}}(\bar{\phi}-\phi)\tilde{D}_n\,\mathrm{d}s+\int_{\Gamma_{ue}}(\bar{u}_z-u_z)\tilde{t}\,\mathrm{d}s-2\int_{\Gamma_{te}}\tilde{u}_z t\,\mathrm{d}s-2\int_{\Gamma_{De}}\tilde{\phi}D_n\,\mathrm{d}s-\int_{\Gamma_{Ie}}(\tilde{\phi}D_n+\tilde{u}_z t\,\mathrm{d}s\Big\} \tag{36b}$$

where

$$\Pi_e^{\sigma D}=\iint_{\Omega_e}H(\sigma_{ij},D_k)\mathrm{d}\Omega+\int_{\Gamma_{ue}}t\bar{u}_z\ \mathrm{d}s+\int_{\Gamma_{\phi e}}D_n\bar{\phi}\,\mathrm{d}s \tag{37a}$$

$$\Pi_e^{\varepsilon E}=\iint_{\Omega_e}H(\varepsilon_{ij},E_k)\mathrm{d}\Omega+\int_{\Gamma_{te}}\bar{t}\tilde{u}_z\,\mathrm{d}s+\int_{\Gamma_{De}}\bar{D}_n\tilde{\phi}\,\mathrm{d}s\ , \tag{37b}$$

$$H(\sigma_{ij},D_k)=-\frac{1}{2}s_{44}(\sigma_{xz}^2+\sigma_{yz}^2)-g_{15}\sigma_{xz}D_x-g_{15}\sigma_{yz}D_y+\frac{1}{2}\lambda_{11}(D_x^2+D_y^2) \tag{38a}$$

$$H(\gamma_{ij},E_k)=\frac{1}{2}c_{44}(\gamma_{xz}^2+\gamma_{yz}^2)-e_{15}\gamma_{xz}E_x-e_{15}\gamma_{yz}E_y-\frac{1}{2}\kappa_{11}(E_x^2+E_y^2) \tag{38b}$$

in which Eq. (13) is assumed to be satisfied, a priori. The terminology "modified principle" refers here to the use of a conventional potential functional ($\Pi_e^{xy}$ here) and some modified terms for the construction of a special variational principle to account for additional requirements such as the condition defined in Eqs. (10) and (11).

The boundary $\Gamma_e$ of a particular element consists of the following parts:

$$\Gamma_e=\Gamma_{ue}\cup\Gamma_{te}\cup\Gamma_{Ie}=\Gamma_{\phi e}\cup\Gamma_{De}\cup\Gamma_{Ie} \tag{39}$$

where

$$\Gamma_{ue}=\Gamma_u\ \cap\ \Gamma_e,\quad \Gamma_{te}=\Gamma_t\ \cap\ \Gamma_e,\quad \Gamma_{\phi e}=\Gamma_\phi\ \cap\ \Gamma_e,\quad \Gamma_{De}=\Gamma_D\ \cap\ \Gamma_e\ , \tag{40}$$

and $\Gamma_{Ie}$ is the inter-element boundary of the element '$e$'. We now show that the stationary condition of the functional (36) leads to Eqs. (6)–(11), and present the theorem on the existence of extremum of the functional, which ensures that an approximate solution can converge to the exact one. These can be mathematically stated as follows:

(a) *Modified complementary principle*

$$\delta\Pi_m^{\sigma D}=0\ \ \Rightarrow\ \ (6)\text{–}(11) \tag{41}$$

where $\delta$ stands for the variation symbol.

(b) *Theorem on the existence of extremum*

If the expression

$$\iint_{\Omega} \delta^2 H \,\mathrm{d}\Omega - \int_{\Gamma_u} \delta t \delta u_z \,\mathrm{d}s - \int_{\Gamma_\phi} \delta D_n \delta\phi \,\mathrm{d}s + \sum_e \int_{\Gamma_{eI}} [(\delta\tilde{\phi} - \delta\phi)\delta D_n + [(\delta\tilde{u}_z - \delta u_z)\delta t] \,\mathrm{d}s \tag{42}$$

is uniformly positive (or negative) at the neighborhood of $\mathbf{u}_0$, where $\mathbf{u}_0$ is such a value that $\Pi_m^{\sigma D}(\mathbf{u}_0) = (\Pi_m^{\sigma D})_0$, and where $(\Pi_m^{\sigma D})_0$ stands for the stationary value of $\Pi_m^{\sigma D}$, we have

$$\Pi_m^{\sigma D} \geq (\Pi_m^{\sigma D})_0 [\text{or } \Pi_m^{\sigma D} \leq (\Pi_m^{\sigma D})_0] \tag{43}$$

in which the relation that $\tilde{\mathbf{u}}_e = \tilde{\mathbf{u}}_f$ is identical on $\Gamma_e \cap \Gamma_f$ has been used.

*Proof:* First, we derive the stationary conditions of functional (36a). To this end, performing a variation of $\Pi_m^{\sigma D}$ and noting that Eq. (13) holds true a priori by the previous assumption, one obtains

$$\delta\Pi_m^{\sigma D} = \int_{\Gamma_u} (\bar{u}_z - u_z)\delta t \,\mathrm{d}s - \int_{\Gamma_t} (\bar{t} - t)\delta\tilde{u}_z \,\mathrm{d}s + \int_{\Gamma_\phi} (\bar{\phi} - \phi)\delta D_n \,\mathrm{d}s - \int_{\Gamma_D} (\bar{D}_n - D_n)\delta\phi \,\mathrm{d}s + \sum_e \int_{\Gamma_{eI}} [(\tilde{u}_z - u_z)\delta t + t\delta\tilde{u}_z + (\tilde{\phi} - \phi)\delta D_n + D_n\delta\tilde{\phi}] \,\mathrm{d}s \tag{44}$$

Therefore, the Euler equations for expression (44) are Eqs. (6)–(11), as the quantities $\delta t, \delta u_z, \delta\tilde{u}_z, \delta D_n, \delta\phi$ and $\delta\phi$ may be arbitrary. The principle (41) has thus been proved. This indicates that the stationary condition of the functional satisfies the required boundary equations and can thus be used for deriving Trefftz displacement element formulation.

As for the proof of the theorem on the existence of extremum, we may complete it by way of the so-called "second variational approach" [31]. In doing this, performing variation of $\delta\Pi_m^{\sigma D}$ and using the constrained conditions (13), we find

$$\delta^2\Pi_m^{\sigma D} = \iint_{\Omega} \delta^2 H \,\mathrm{d}\Omega - \int_{\Gamma_u} \delta t \delta u_z \,\mathrm{d}s - \int_{\Gamma_\phi} \delta D_n \delta\phi \,\mathrm{d}s + \sum_e \int_{\Gamma_{eI}} [(\delta\tilde{\phi} - \delta\phi)\delta D_n + (\delta\tilde{u}_z - \delta u_z)\delta t] \,\mathrm{d}s = \text{expression (42)} \tag{45}$$

Therefore the theorem has been proved from the sufficient condition of the existence of a local extreme of a functional [31]. This completes the proof.

## 4 Generation of element matrix

The element matrix may be established by setting $\delta\Pi_{me}^{\sigma D} = 0$ or $\delta\Pi_{me}^{\varepsilon E} = 0$. As an illustration, we use $\delta\Pi_{me}^{\sigma D} = 0$ to derive the element stiffness matrix. To simplify the derivation, the domain integral in (37) is converted into a boundary one by use of solution properties of the intraelement trial functions, for which the functional (36) is rewritten as

$$\Pi_{me}^{\sigma D} = -\int_{\Gamma_{De}} (\bar{D}_n - D_n)\tilde{\phi} \,\mathrm{d}s - \int_{\Gamma_{te}} (\bar{t} - t)\tilde{u}_z \,\mathrm{d}s + \int_{\Gamma_{Ie}} (D_n\tilde{\phi} + t\tilde{u}_z) \,\mathrm{d}s - \frac{1}{2}\int_{\Gamma_e} (tu_z + D_n\phi) \,\mathrm{d}s + \int_{\Gamma_{ue}} t\bar{u}_z \,\mathrm{d}s + \int_{\Gamma_{\phi e}} D_n\bar{\phi} \,\mathrm{d}s \tag{46}$$

Substituting the expressions given in Eqs. (18) and (20) into (23) produces

$$\Pi_{me}^{\sigma D} = -\frac{1}{2}\mathbf{c}^{\mathrm{T}}\mathbf{H}\mathbf{c} + \mathbf{c}^{\mathrm{T}}\mathbf{S}\mathbf{d} + \mathbf{c}^{\mathrm{T}}\mathbf{r}_1 + \mathbf{d}^{\mathrm{T}}\mathbf{r}_2 + \text{terms without } \mathbf{c} \text{ or } \mathbf{d} \tag{47}$$

in which the matrices $\mathbf{H}$, $\mathbf{S}$ and the vectors $\mathbf{r}_1$, $\mathbf{r}_2$ are defined by

$$\begin{aligned} \mathbf{H} &= \int_{\Gamma_e} \mathbf{Q}^{\mathrm{T}}\mathbf{N} \,\mathrm{d}s \\ \mathbf{S} &= \int_{\Gamma_{De}} \mathbf{Q}_2^T\tilde{\mathbf{N}}_2 \,\mathrm{d}s + \int_{\Gamma_{te}} \mathbf{Q}_1^T\tilde{\mathbf{N}}_1 \,\mathrm{d}s + \int_{\Gamma_{Ie}} \mathbf{Q}^T\tilde{\mathbf{N}} \,\mathrm{d}s \\ \mathbf{r}_1 &= \int_{\Gamma_{\phi e}} \mathbf{Q}_2^T\bar{\phi} \,\mathrm{d}s + \int_{\Gamma_{ue}} \mathbf{Q}_1^T\bar{u}_z \,\mathrm{d}s \\ \mathbf{r}_2 &= -\int_{\Gamma_{De}} \tilde{\mathbf{N}}_2^T\bar{D}_n \,\mathrm{d}s - \int_{\Gamma_{te}} \tilde{\mathbf{N}}_1^T\bar{t} \,\mathrm{d}s \ . \end{aligned} \tag{48}$$

The symmetry of the matrix $\mathbf{H}$ can be shown by considering the generalized energy $U_e$ of a particular element 'e':

$$\begin{aligned} 2U_e &= 2\iint_{\Omega_e} H(\sigma_{ij}, D_k) \,\mathrm{d}\Omega = \iint_{\Omega_e} (-\sigma_{ij}\gamma_{ij} + D_kE_k) \,\mathrm{d}\Omega \\ &= -\int_{\Gamma_e} (\sigma_{ij}n_ju_i + D_in_i\phi) \,\mathrm{d}s \\ &= -\int_{\Gamma_e} \mathbf{T}^{\mathrm{T}}\mathbf{u} \,\mathrm{d}s = -\int_{\Gamma_e} \mathbf{u}^{\mathrm{T}}\mathbf{T} \,\mathrm{d}s \end{aligned} \tag{49}$$

where

$$\int_{\Gamma_e} \mathbf{T}^{\mathrm{T}}\mathbf{u} \,\mathrm{d}s = \mathbf{c}^{\mathrm{T}} \left[\int_{\Gamma_e} \mathbf{Q}^{\mathrm{T}}\mathbf{N} \,\mathrm{d}s\right] \mathbf{c} = \mathbf{c}^{\mathrm{T}}\mathbf{H}\mathbf{c} \tag{50}$$

$$\int_{\Gamma_e} \mathbf{u}^{\mathrm{T}}\mathbf{T}\,\mathrm{d}s = \mathbf{c}^{\mathrm{T}}\left[\int_{\Gamma_e} \mathbf{N}^{\mathrm{T}}\mathbf{Q}\,\mathrm{d}s\right]\mathbf{c} = \mathbf{c}^{\mathrm{T}}\mathbf{H}^{\mathrm{T}}\mathbf{c} \tag{51}$$

Therefore $\mathbf{H} = \mathbf{H}^{\mathrm{T}}$.

To enforce inter-element continuity on the common element boundary, the unknown vector $\mathbf{c}$ should be expressed in terms of nodal degrees of freedom $\mathbf{d}$. An optional relationship between $\mathbf{c}$ and $\mathbf{d}$ in the sense of variation can be obtained from



$$\frac{\partial \Pi_{me}^{\sigma D}}{\partial \mathbf{c}^{\mathrm{T}}} = -\mathbf{H}\mathbf{c} + \mathbf{S}\mathbf{d} + \mathbf{r}_1 = 0 \ . \tag{52}$$

This leads to

$$\mathbf{c} = \mathbf{G}\mathbf{d} + \mathbf{g} \ , \tag{53}$$

where $\mathbf{G} = \mathbf{H}^{-1}\mathbf{S}$ and $\mathbf{g} = \mathbf{H}^{-1}\mathbf{r}_1$, and then straightforwardly yields the expression of $\Pi_{me}^{\sigma D}$ only in terms of $\mathbf{d}$ and other known matrices

$$\Pi_{me}^{\sigma D} = \frac{1}{2}\mathbf{d}^{\mathrm{T}}\mathbf{G}^{\mathrm{T}}\mathbf{H}\mathbf{G}\mathbf{d} + \mathbf{d}^{\mathrm{T}}(\mathbf{G}^{\mathrm{T}}\mathbf{H}\mathbf{g} + \mathbf{r}_2) + \text{terms without } \mathbf{d} \ . \tag{54}$$

Therefore, the element stiffness matrix equation can be obtained by taking the vanishing variation of the functional $\Pi_{me}^{\sigma D}$ as

$$\frac{\partial \Pi_{me}^{\sigma D}}{\partial \mathbf{d}^{\mathrm{T}}} = 0 \quad \Rightarrow \quad \mathbf{K}\mathbf{d} = \mathbf{P} \tag{55}$$

where $\mathbf{K} = \mathbf{G}^{\mathrm{T}}\mathbf{H}\mathbf{G}$ and $\mathbf{P} = -\mathbf{G}^{\mathrm{T}}\mathbf{H}\mathbf{g} - \mathbf{r}_2$ are, respectively, the element stiffness matrix and the equivalent nodal flow vector. The expression (55) is the elemental stiffness matrix equation for Trefftz FE analysis.

## 5
## Numerical examples

As a numerical illustration of the proposed formulation we consider an anti-plane crack of length $2c$ embedded in an infinite PZT-5H medium which is subjected to a uniform shear traction, $\sigma_{zy} = \tau_\infty$, and a uniform electric displacement, $D_y = D_\infty$ at infinity (see Fig. 3). The material properties of PZT-5H are as given by [32]: $c_{44} = 3.53 \times 10^{10}\,\mathrm{N/m^2}, e_{15} = 17.0\,\mathrm{C/m^2}, \kappa_{11} = 1.51 \times 10^{-8}\,\mathrm{C/(Vm)}, J_{\mathrm{cr}} = 5.0\,\mathrm{N/m}$, where $J_{\mathrm{cr}}$ is the critical energy release rate. In our FE analysis, one half of the geometry configuration shown in Fig. 4 is used and a typical element mesh is shown in Fig. 5. However, duo to the symmetry about $x$-axis (the line AB in Fig. 5), only one half of the mesh in Fig. 5 has been used, actually. Since the trial functions the crack element satisfy the crack face condition and represent the singularity at crack tip, it is unnecessary to increase the mesh density near the crack tip. In the calculation, three types of element (see Fig. 5) has been used. The energy release rate for PZT-5H material with a crack of length $2c$ =0.02 m and $a/c = 15$ is plotted in Fig. 6 as a function of electrical load with the mechanical load fixed such that $J = J_{\mathrm{cr}}$ at zero electric load. The results are compared with those from Ref. [33]. It is found from Fig. 6 that the energy release rate can be negative which means the crack growth may be arrested.

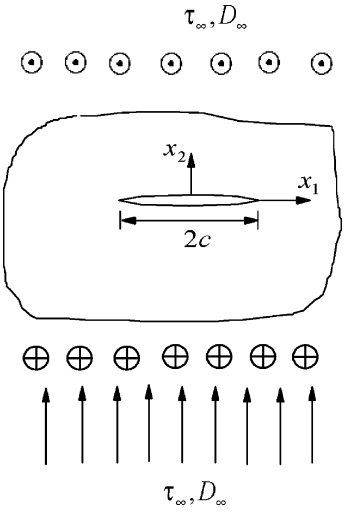


**Fig. 3.** Configuration of the cracked infinite piezoelectric medium

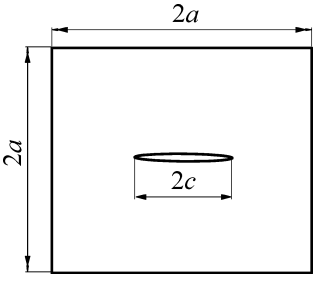


**Fig. 4.** Geometry of the cracked solid in finite element analysis

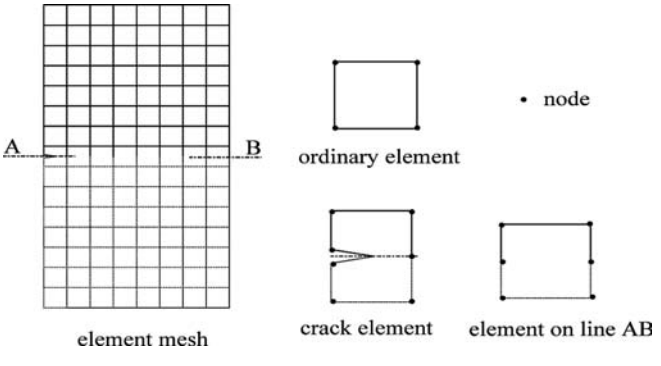


**Fig. 5.** A typical element mesh and element types

To study the convergent performance of the proposed formulation, numerical results for different element meshes $8 \times 8, 12 \times 12, 16 \times 16, 20 \times 20$, and $24 \times 24$ are presented in Table 1 that the $h$-extension performs very nicely, and Table 2 shows the results of $J/J_{\mathrm{cr}}$ versus $M$, here $2M$ is the number of hierarchic degrees of freedom. It also shows a good convergent performance.

The boundary effect is investigated by using different ratios of $a/c$ (=5, 7, 10, 12, and 15). Numerical results of $J/J_{\mathrm{cr}}$ for different a/c are listed in Table 3. We find that the accuracy of the results is adequate when $a/c$ is greater than 10.

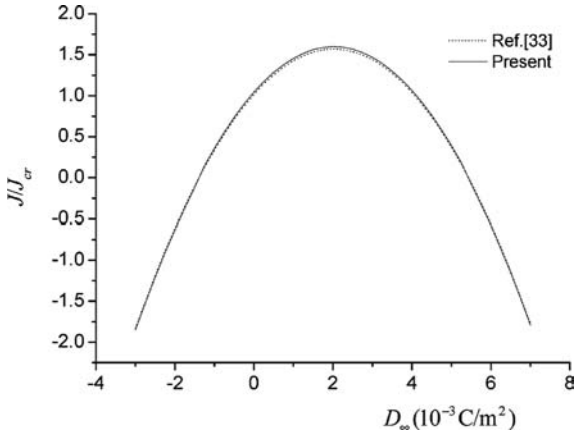


**Fig. 6.** Energy release rate in cracked PZT-5H plate ($a/c = 15, 24 \times 24$, and $\tau_\infty = 4.2 \times 10^6\ \mathrm{N/m^2}$)

**Table 1.** $h$-convergence study for $J/J_{cr}$ for the central cracked piezoelectric plate ($a/c = 15$, $D_\infty = 2 \times 10^{-3}\mathrm{C/m^3}$, and $\tau_\infty = 4.2 \times 10^6\ \mathrm{N/m^2}$)

| Meshes | $J/J_{cr}$ |
|---|---|
| $8 \times 8$ | 1.5954 |
| $12 \times 12$ | 1.5908 |
| $16 \times 16$ | 1.5899 |
| $20 \times 20$ | 1.5895 |
| $24 \times 24$ | 1.5893 |

**Table 2.** $p$-convergence study for $J/J_{cr}$ for the central cracked piezoelectric plate ($a/c = 15$, $16 \times 16$, $D_\infty = 2 \times 10^{-3}\ \mathrm{C/m^3}$, and $\tau_\infty = 4.2 \times 10^6\ \mathrm{N/m^2}$)

| $M$ | $J/J_{cr}$ |
|---|---|
| 0 | 1.5899 |
| 1 | 1.5896 |
| 2 | 1.5895 |
| 3 | 1.5894 |

**Table 3.** Boundary effect study on $J/J_{cr}$ for central cracked piezoelectric plate ($24 \times 24$, $D_\infty = 2 \times 10^{-3}\ \mathrm{C/m^3}$, and $\tau_\infty = 4.2 \times 10^6\ \mathrm{N/m^2}$)

| $a/c$ | $J/J_{cr}$ |
|---|---|
| 5 | 1.5968 |
| 7 | 1.5917 |
| 10 | 1.5898 |
| 12 | 1.5894 |
| 15 | 1.5893 |

## 6 Conclusions

A dual modified variational formulation is developed for Trefftz FE analysis anti-plane piezoelectric materials. Based on the assumed intraelement and frame fields as well as the newly constructed dual variational functional, an element stiffness matrix equation is obtained which can easily be implemented into computer programs for numerical analysis with the Trefftz FE method. On the basis of the formulas presented and the theoretical model in [32, 33], a numerical example has been calculated with several FE meshes. The discrepancy between the two models is within 2% and the results converge gradually to the analytical result when the mesh density is increased.

## References


1. **Jirousek J, Leon N** (1977) A powerful finite element for plate bending. Comput. Meth. Appl. Mech. Eng. 12: 77–96
2. **Jirousek J, Venkatesh A** (1992) Hybrid-Trefftz plane elasticity elements with $p$-method capabilities. Int. J. Numer. Meth. Eng. 35: 1443–1472
3. **Piltner R** (1985) Special finite elements with holes and internal cracks. Int. J. Numer. Meth. Eng. 21: 1471–1485
4. **Jirousek J, Guex L** (1986) The hybrid-Trefftz finite element model and its application to plate bending. Int. J. Numer. Meth. Eng. 23: 651–693
5. **Qin QH** (1994) Hybrid Trefftz finite element approach for plate bending on an elastic foundation. Appl. Math. Modelling 18: 334–339
6. **Jin FS, Qin QH** (1995) A variational principle and hybrid Trefftz finite element for the analysis of Reissner plates. Comput. Struct. 56: 697–701
7. **Jirousek J, Wroblewski A, Qin QH, He XQ** (1995) A family of quadrilateral hybrid Trefftz $p$-element for thick plate analysis. Comput. Meth. Appl. Mech. Eng. 127: 315–344
8. **Qin QH** (1995) Hybrid Trefftz finite element method for Reissner plates on an elastic foundation. Comput. Meth. Appl. Mech. Eng. 122: 379–392
9. **Piltner R** (1992) A quadrilateral hybrid-Trefftz plate bending element for the inclusion of warping based on a three-dimensional plate formulation. Int. J. Numer. Meth. Eng. 33: 387–408
10. **Piltner R** (1989) On the representation of three-dimensional elasticity solutions with the aid of complex value functions. J. Elasticity 22: 45–55
11. **Stein E, Peters K** (1991) A new boundary-type finite element for 2D and 3D elastic solids. In: Onate E, Periaux J, Samuelson A (eds) The Finite Element Method in the 1990s, a book dedicated to O.C. Zienkiewicz, Springer: Berlin, pp. 35–48
12. **Wroblewski A, Zielinski AP, Jirousek J** (1992) Hybrid-Trefftz p-element for 3-D axisymmetric problems of elasticity. In: Hirsch C, Zienkiewicz OC, Onãte E (eds) Numerical methods in Engineering'92, Proc. First Europ. Conf. On Numer. Meth. in Eng. Elsevier: Brussel, pp. 803–810
13. **Jirousek J, Stojek M** (1995) Numerical assessment of a new T-element approach. Comput. Struct. 57: 367–378
14. **Zielinski AP, Zienkiewicz OC** (1985) Generalized finite element analysis with T-complete boundary solution functions. Int. J. Numer. Meth. Eng. 21: 509–528
15. **Vörös GM, Jirousek J** (1991) Application of the hybrid-Trefftz finite element model to thin shell analysis. In: Ladeveze P, Zienkiewicz OC (eds) Proc. Europ. Conf. on new Advances in Comput. Struc. Mech. Giens, France, Elsevier, pp. 547–554
16. **Freitas JAT** (1997) Hybrid-Trefftz displacement and stress elements for elasto-dynamic analysis in the frequency domain. Comput. Assisted Mech. Eng. Sci. 4: 345–368
17. **Markiewicz M, Mahrenholtz O** (1997) Combined time-stepping and Trefftz approach for nonlinear wave-structure interaction. Comput. Assisted Mech. Eng. Sci. 4: 567–586
18. **Qin QH** (1996) Transient plate bending analysis by hybrid Trefftz element approach. Commun. Numer. Meth. Eng. 12: 609–616
19. **Jirousek J, Qin QH** (1996) Application of Hybrid-Trefftz element approach to transient heat conduction analysis. Comput. Struct. 58: 195–201

**20. Qin QH** (1995) Postbuckling analysis of thin plates by a hybrid Trefftz finite element method. Comput. Meth. Appl. Mech. Eng. 128: 123–136
**21. Qin QH** (1996) Nonlinear analysis of thick plates by HT FE approach. Comput. Struct. 61: 271–281
**22. Qin QH** (1997) Postbuckling analysis of thin plates on an elastic foundation by HT FE approach. Appl. Math. Modelling 21: 547–556
**23. Qin QH, Diao S** (1996) Nonlinear analysis of thick plates on an elastic foundation by HT FE with *p*-extension capabilities. Int. J. Solids Struct. 33: 4583–4604
**24. Freitas JAT, Wang ZM** (1998) Hybrid-Trefftz stress elements for elastoplasticity. Int. J. Numer. Meth. Eng. 43: 655–683
**25. Zielinski AP** (1988) Trefftz method: elastic and elastoplastic problems. Comput. Meth. Appl. Mech. Eng. 69: 185–204
**26. Jirousek J, Teodorescu P** (1982) Large finite elements method for the solution of problems in the theory of elasticity. Comput. Struct. 15: 575–587
**27. Venkatesh A, Jirousek J** (1995) Accurate representation of local effect due to concentrated and discontinuous loads in hybrid-Trefftz plate bending elements. Comput. Struct. 57: 863–870
**28. Sabino J, Portela A, Castro PMST de** (1999) Trefftz boundary element method applied to fracture mechanics. Eng. Frac. Mech. 64: 67–86
**29. Freitas JAT, Ji ZY** (1996) Hybrid-Trefftz equilibrium model for crack problems. Int. J. Numer. Meth. Eng. 39: 569–584
**30. Qin QH** (2000) The Trefftz Finite and Bound. Elem. Method, WIT Press, Southampton
**31. Simpson HC, Spector SJ** (1987) On the positive of the second variation of finite elasticity. Arch. Rational Mech. Anal. 98: 1–30
**32. Pak YE** (1990) Crack extension force in a piezoelectric material. J. Appl. Mech. 57: 647–653
**33. Qin QH** (2001) Fracture Mechanics of Piezoelectric Materials, WIT Press, Southampton